Effects of geomagnetic disturbances on linear growth rate of collisional Rayleigh-Taylor Instability during solar maximum

Chien-Chih Lee

General Education Center, Ching Yun University,
No.229, Jianxing Road, Zhongli City, Taoyuan County 32097, Taiwan
cclee@cyu.edu.tw

Abstract

This study chooses 3 cases under geomagnetic disturbed conditions to investigate the effects of geomagnetic disturbance on local linear growth rate (γ) of collisional Rayleigh-Taylor (CR-T) instability. In the case at 30 July 1999, the γ value is 2.6 times the associated quiet-condition reference value. In contrast, at 12 September 1999, the γ value is obviously smaller than the associated quiet-condition reference value. In addition, the growth rates in the case of 26 September 1999 are not affected by the geomagnetic disturbances. The γ values are close to the associated quiet-condition reference value.

1. Introduction

For five decades, the Rayleigh-Taylor (R-T) instability has been accepted to be the major mechanism of the equatorial spread F (ESF) [1-3]. Now, it is known that the ESF generation mainly depends on three basic factors: (1) linear growth rate for R-T instability, (2) flux-tube-integrated Pedersen conductivity that controls the nonlinear development, and (3) density perturbations to serve as seeding sources [4]. Among these factors, the growth rate in the theory of R-T instability might be the most important factor [2, 4, 5]. In the previous studies, the linear growth rate in local and flux-tube-integrated quantities have been applied on the theoretical and experimental works [2, 3, 5, 6].

To understand how the geomagnetic disturbance modifies the growth rate, this work examines the linear growth rate under geomagnetic disturbed conditions. The estimation of growth rate is based on the local linear growth rate of CR-T instability [6]. The definition of geomagnetic disturbed conditions is that the average *Kp* of interval of 1800-2400 UT (1300-1900 LT) is greater than or equal to 5 [7-9]. According to this definition, there are 3 cases in April 1999-March 2000, close to the solar maximum, selected in this study.

2. Data analysis

The equation of local linear growth rate (γ) is introduced by [6], as

$$\gamma = \frac{1}{n_0}\frac{\partial n_0}{\partial h}\frac{g}{\nu} - R \quad \sec^{-1}. \tag{1}$$

978-1-4244-5118-0/11/$26.00 ©2011 IEEE

In equation (1), the n_0 is the background electron density, h is the height above the Earth, ν is the ion-neutral collision frequency, g is gravity (positive downward), and R is the local recombination rate. The $(n_0)(\partial h/\partial n_0)$ is defined as the gradient density scale length (L) of the background electron density profile. The value of L in equation (1) is obtained from the electron profile observed by the Jicamarca digisonde (12°S, 76.9°W, dip latitude: 1.2°N), near the dip equator. It is noted that the electron profile and F2-peak height (hmF2) are derived from the Jicamarca ionogram using the true height inversion algorithm NHPC [10] imbedded in the SAO explorer software package [11]. The values of ν and R are derived from the atmospheric quantities modeled by MSISE-90 model [12]. The estimation procedure of this growth rate is described in Lee (2006) in detail. Since the purpose of this study is to reveal the geomagnetic disturbed effects on growth rate, the data of days on which the average *Kp* of interval of 1300-1900 LT is greater than or equal to 5 during April 1999-March 2000 are selected. In addition, the monthly averages of hmF2, deduced from the geomagnetic quiet days, is used to be the quiet-condition reference values.

3. Results and discussion

3.1 Case 1: 30 July 1999

First, the growth rates in the sunset period of 30 July 1999 are examined. The Kp values are 7.7 and 6.3 at 1300-1600 LT and 1600-1900 LT of 30 July, respectively. Figure 1a shows the altitude profiles of γ at 1600 (solid line), 1700 (dotted line), 1800 (dashed line), and 1900 (dash-dot line) LT of 30 July 1999. It is found in Figure 1a that the values of γ profile at 1900 LT are obviously largest. For the profile at 1900 LT, the greatest γ value is 8.7×10^{-4} sec^{-1} at 399.4 km. This γ value is much larger than the average γ value of July 1999 (3.3×10^{-4} sec^{-1}), even larger than that in April (7.8×10^{-4} sec^{-1}) and October (7.3×10^{-4} sec^{-1}) 1999 [5] It is noted that the ESF occurs frequently in April and October (77% and 84%) [9]. Therefore, the γ value of 8.7×10^{-4} sec^{-1} would help the ESF occurring from 1930 LT of 30 July to 0300 LT of 31 July (shown in Figure 1b). Moreover, the larger γ value in this case is related to the enhanced uplift in hmF2 at 1900 LT (Figure 1b), because the γ value is positively correlated to the hmF2 [5]. The hmF2 at 1900 LT of 30 July (bold line) is higher than the quiet-conditions reference value of July (dashed line) by 30 km.

3.2 Cases 2: 12 September 1999

Next, the growth rates of two days, in which the ESF does not occur in the sunset period, are examined. It is noted that these two days are in September, in which the ESF occurrence is high (81%) [9]. For the case of 12 September 1999, the Kp values are 6 and 5 at 1300-1600 LT and 1600-1900 LT of 12 September, respectively. In Figure 2a, the γ profiles at 1800 (dashed line) and 1900 (dash-dot line) LT at 12 September are presented. It is noted that in Figure 2a, the γ profiles at 1600, 1700, and 2000 LT are not shown because of the negative γ values. The negative γ values are because the value of R is larger than that of g/Lν, while the F2-peak height (hmF2) is lower (Figure 2b).

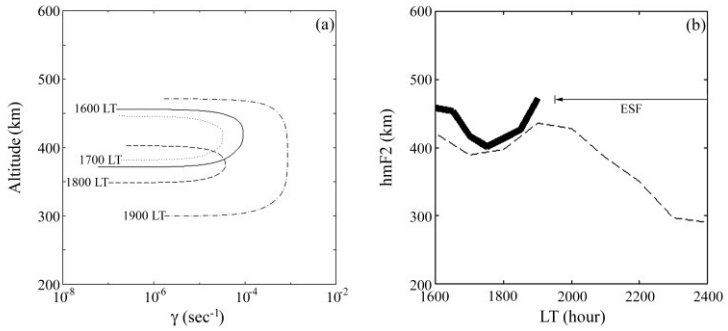

Figure 1. (a) The γ profiles at 1600 (solid line), 1700 (dotted line), 1800 (dashed line), and 1900 (dash-dot line) LT of 30 July 1999. (b) The hmF2 during 1600-2400 LT of 30 July 1999 (bold line) and the associated quiet-condition reference values (dashed line).

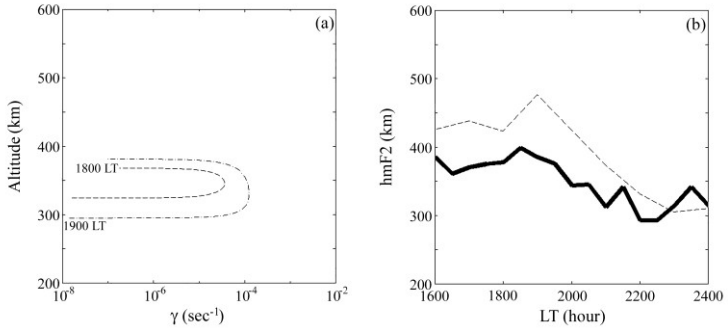

Figure 2. (a) The γ profiles at 1800 (dashed line), and 1900 (dash-dot line) LT of 12 September 1999. (b) The hmF2 during 1600-2400 LT of 30 July 1999 (bold line) and the associated quiet-condition reference values (dashed line).

3.3 Cases 4-5: 26 September 1999

In addition to the cases for γ increase/decrease, there are two other cases which are not influenced by the geomagnetic disturbances. For one case at 26 September 1999, the Kp values are 4.7 and 5.3 at 1300-1600 LT and 1600-1900 LT, respectively. Figure 3a shows the γ profiles at 1600 (solid line), 1700 (dotted line), 1800 (dashed line), and 1900 (dash-dot line) LT of 26 September 1999. In this figure, the value and altitude range of γ profiles increase from 1600 to 1900 LT. This variation is associated to the hmF2 variation (Figure 3b), which rises from 1600 to 1900 LT. Additionally, the hmF2 values during 1600-1930 LT of 26 September 1999 (bold line) are similar to the quiet-condition reference values (dashed line). The profiles of γ and associated parameters at 1900 LT of 26 September 1999 are close to the reference values. Because of the higher ESF occurrence (81%) in September, it is expectable that the ESF appears during 2000-2300 LT on 26 September 1999.

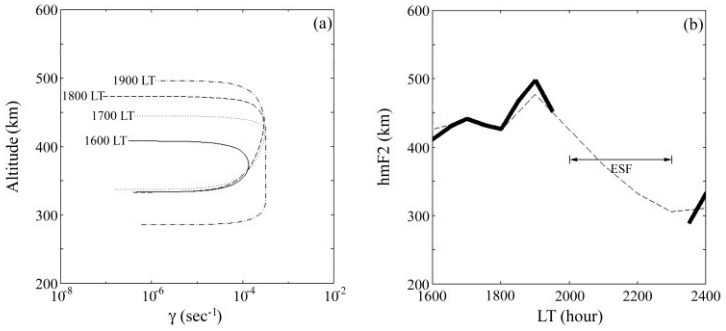

Figure 3. (a) The γ profiles at 1600 (solid line), 1700 (dotted line), 1800 (dashed line), and 1900 (dash-dot line) LT of 26 September 1999. (b) The hmF2 during 1600-2400 LT of 26 September 1999 (bold line) and the associated quiet-condition reference values (dashed line).

4. References

1. S. L. Ossakow, Spread F theories-a review, *J. Atmos. Terr. Phys.*, 1981, 437-452.

2. P. J. Sultan, Linear theory and modeling of the Rayleigh-Taylor instability leading to the occurrence of equatorial spread F, *J. Geophys. Res.*, 1996, 26875-26891.

3. M. C. Kelley, *The Earth's Ionosphere*, Int. Geophys. Ser., vol. 43, Elsevier, New York, 1989.

4. M. A. Abdu, Outstanding problems in the equatorial ionosphere-thermosphere electrodynamics relevant to spread F, *J. Atmos. Solar-Terr. Phys.*, 2001, 869-884.

5. C. C. Lee, Examine the local linear growth rate of collisional Rayleigh-Taylor instability during solar maximum, *J. Geophys. Res.*, 2006, doi:10.1029/2006JA011925.

6. S. L. Ossakow, S. T. Zalesak, and B. E. McDonald, Nonlinear equatorial spread F: Dependence on altitude of the F peak and bottomside background electron density gradient scale length, *J. Geophys. Res.*, 1979, 17-29.

7. B. G. Fejer, L. Scherliess, and E. R. de Paula, Effects of the vertical plasma drift velocity on the generation and evolution of equatorial F, *J. Geophys. Res.*, 1999, 19859-19869.

8. C. C. Lee, S. Y. Su, and B. W. Reinisch, Concurrent study of bottomside spread F and plasma bubbles using digisonde and ROCSAT-1 in the equatorial ionosphere during solar maximum, *Ann. Geophys.*, 2005, 3473-3480.

9. C. C. Lee, J. Y. Liu, B. W. Reinisch, and W. S. Chen, and F. D. Chu, The effects of the pre-reversal E×B drift, the EIA asymmetry, and geomagnetic activity on the equatorial spread F during solar maximum, *Ann. Geophys.*, 2005, 745-751.

10. X. Huang, and B W. Reinisch, Vertical electron content from ionograms in real time, *Radio Sci.*, 2001, 335-342.

11. B. W. Reinisch, Modern ionosondes, in *Modern Radio Science*, (edited by H. Kohl, R. Ruester, and K. Schlegel), European Geophysical Society, Katlenburg-Lindau, Germany, 1996, pp. 440-458.

12. A. E. Hedin, Extension of the MSIS thermospheric model into the middle and lower atmosphere, *J. Geophys. Res.*, 1991, 1159-1172.